Toggling Between Blue- and Red-Emitting Fluorescent Silver Nanoclusters

ARTICLE *in* JOURNAL OF PHYSICAL CHEMISTRY LETTERS · NOVEMBER 2012

Impact Factor: 7.46 · DOI: 10.1021/jz301733y

3 AUTHORS:

Uttam Anand
University of Alberta
18 PUBLICATIONS **246** CITATIONS
SEE PROFILE

Subhadip Ghosh
Indian Institute of Science Education and Re…
12 PUBLICATIONS **57** CITATIONS
SEE PROFILE

Saptarshi Mukherjee
Indian Institute of Science Education and Re…
49 PUBLICATIONS **639** CITATIONS
SEE PROFILE

THE JOURNAL OF PHYSICAL CHEMISTRY Letters

Letter

pubs.acs.org/JPCL

Toggling Between Blue- and Red-Emitting Fluorescent Silver Nanoclusters

Uttam Anand,[§] Subhadip Ghosh,[§] and Saptarshi Mukherjee*

Department of Chemistry, Indian Institute of Science Education and Research Bhopal, ITI Campus (Gas Rahat) Building, Govindpura, Bhopal 462 023, Madhya Pradesh, India

Supporting Information

ABSTRACT: A very efficient protocol for synthesizing highly fluorescent, protein-templated silver nanoclusters (Ag/NCs) has been discussed. Two types of Ag/NCs (Ag_9/HSA and Ag_{14}/HSA), although showing significant differences in their photophysical properties, can be interconverted at will, which makes this study unique. The Ag/HSA NCs have been quantified by several spectroscopic techniques, and they find tremendous applications as photoluminescent markers. Besides their rather easy synthetic methodology, our Ag/HSA NCs show two-photon excitation properties that enable them to be used in bioimaging.

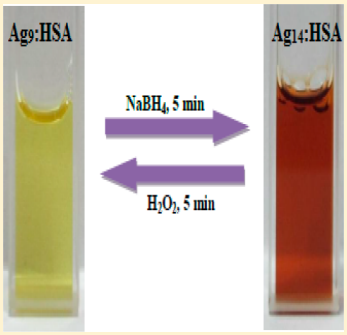

SECTION: Physical Processes in Nanomaterials and Nanostructures

Synthesis, characterization, and applications of noble metal nanoclusters (NCs), assisted by the presence of a protein template, have been topics of burgeoning interests of late.[1−3] Besides having an excellent photostability, photoluminescence, and large Stokes shifts, these NCs are characterized by having very low toxicity as compared to quantum dots.[4,5] Among several noble metal nanoparticles[6−8] and NCs, Ag/NCs occupy a seminal position as they prove to be excellent fluorophores for optical biolabeling, sensing, and imaging even at single-molecule resolution.[9] The size regime of these NCs (typically <1 nm) is comparable to the Fermi wavelength of conduction electrons and results in discrete electronic transitions and size-dependent fluorescence, thus exhibiting superior optical, electrical, and biomedical properties compared to larger metal nanoparticles.[1,3,10,11] Silver NCs with a varying number of Ag atoms have been synthesized, and these have been reported to have electronic transitions in the range of 400−700 nm.[1,12−14] Synthetic methods for the preparation of noble metal NCs using various templated assemblies such as DNA,[15] polypeptides,[12,16] polymers,[17] dendrimers,[18] proteins,[1,3,14] thiols,[19] and so forth have been documented. Although these methods could obtain fluorescent NCs, there were drawbacks in terms of relatively low quantum yield (QY) and stability and formation of larger sized nanoclusters or even nanoparticles as a side product. Au/NCs having luminescent properties in the blue to near-IR regimes have been reported, but the QYs are extremely low.[19−21] Using poly(amidoamine) dendrimer templates, Dickson and co-workers[10,11] have synthesized Au/NCs having QYs greater than 10%. Similar values of QYs have also been reported for Ag/NCs,[1] and hence, it is always a real challenge to increase the fluorescent properties of these NCs so that they can more effectively be used for clinical applications.

In order to overcome the shortcomings of the luminescent properties of NCs as mentioned above, herein we report a protein-mediated synthesis of two highly fluorescent silver NCs, one synthesized by a green and nontoxic method (Ag_9/HSA) and another by the conventional $NaBH_4$ reduction (Ag_{14}/HSA). For both syntheses, we used a circulatory protein, human serum albumin (HSA), as a template at the physiological temperature of 37 °C. The important features of Ag_9/HSA are (i) one-pot, green synthesis having blue emission centered at 460 nm, which is stable for more than 3 months, (ii) higher QYs using a protein template (16%) and high fluorescence lifetime (7.51 ns), and (iii) further reduction gives red nanoclusters (emission at 690 nm), which can further be reoxidized to Ag_9/HSA with almost 100% recovery. The important features of Ag_{14}/HSA are (i) higher QYs using a protein template (11%) and fluorescence lifetime (2.72 ns) and (ii) oxidation gives Ag_9/HSA NCs (emission at 460 nm), which can further be reduced to red-emitting NCs. The novelty of this present study is that we can interconvert both Ag/HSA NCs (depending on the experimental conditions) at will and as per our need.

A typical Ag_9/HSA was synthesized by adding aqueous $AgNO_3$ (5 mL, 10 mM) solution to a HSA solution (5 mL, 0.75 mM) under vigorous stirring followed by the addition of a NaOH (0.3 mL, 1000 mM) solution after 2 min. The pH of the reaction mixture was ∼11, and at this pH, the reducing capability of HSA (from the 18 tyrosine residues) became

Received: October 26, 2012
Accepted: November 26, 2012

   dx.doi.org/10.1021/jz301733y | J. Phys. Chem. Lett. 2012, 3, 3605−3609

activated. The mixture was incubated at 37 °C for 10 h, and the fluorescence intensity exhibited by the yellow solution of Ag_9/HSA remained steady (monitored for 3 months). The Ag_{14}/HSA were synthesized by adding $NaBH_4$ (10 mM) to a mixture of an aqueous solution containing $AgNO_3$ (5 mL, 10 mM), HSA (5 mL, 0.75 mM), and NaOH (0.3 mL, 1000 mM) under vigorous stirring. The 10 mM $NaBH_4$ solution was added dropwise until a reddish-brown color was obtained. It must be mentioned here that the synthesis of Ag_{14}/HSA is achieved very quickly (within 2 min) as compared to Ag_9/HSA, which takes about 10 h. The detailed procedure of syntheses for both NCs and the instrumentation used are mentioned in the Supporting Information (SI).

The absorption spectra of HSA alone have a peak centered at 278 nm, and the nature of the absorption changes when Ag/HSA NCs are formed (Figure S1, SI). For both NCs, the absorption spectra are rather broad, and the absorbance profiles are markedly different from that of HSA alone. These broad spectra having small red-shifted humps (as compared to HSA alone) are signatures of the formation of the two NCs in solution. The emission spectra (Figure 1) for Ag_9/HSA (λ_{ex} = 380 nm) and Ag_{14}/HSA (λ_{ex} = 480 nm) NCs were peaked at 460 (QY of 16%) and 620 nm (QY of 11%; please see the SI for details), respectively.

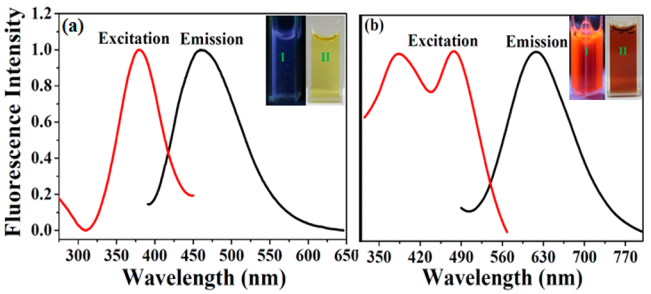

Figure 1. Normalized excitation and emission spectra of (a) Ag_9/HSA and (b) Ag_{14}/HSA; I and II (inset) correspond to the photographs taken under UV and ordinary white light, respectively.

The QYs for NCs using protein as a template, mentioned herein, are one of the highest obtained to date, which corroborates the efficiency of the synthetic procedures that we employed. In order to have a better understanding of the excited-state dynamics, we performed picosecond time-resolved measurements for both Ag/HSA systems. The average lifetimes for Ag_9/HSA and Ag_{14}/HSA were 7.51 [2.35 (26.8%), 10.8 (63.2%), and 0.47 ns (10%)] and 2.72 ns, [1.71 (42.4%), 5.18 (36.8%), and 0.45 ns (20.8%)], respectively (Figure 2 and Table 1). Although the lifetimes reported herein are high, higher lifetime values of Ag NCs have been reported.[22] In a very seminal work, Banerjee and co-workers[22] have studied water-soluble fluorescent Ag NCs using a small molecule, dihydrolipoic acid, and have reported that these Ag NCs have a very high photoluminescence lifetime of 39.96 μs.

This variation of lifetimes can be explained from the energy gap law.[11,23] The lifetimes of the NCs are dependent on both radiative (Γ) and nonradiative (k_{nr}) decay rates, and the value of k_{nr} increases as the emission energy decreases. In our present case, the Ag_{14}/HSA have lower energies (having the emission maximum at 620 nm), and consequently, the magnitude of k_{nr} is higher, which makes the lifetime shorter as compared to Ag_9/HSA. Also, the rotational anisotropy times (τ_{rot}) for both NCs

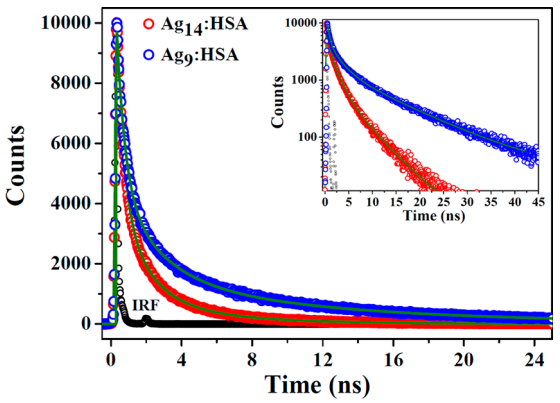

Figure 2. Fluorescence lifetime decays for Ag_9/HSA and Ag_{14}/HSA. The scattered red and blue points represent the actual decay profiles, while the solid green lines represent a triexponential fit to that decay. The IRF is the instrument response function, that is, the contribution from the laser diodes that was deconvulated after fitting. Because the IRFs from both laser diode sources (N-375L and N-470L) were almost similar, the IRF for the N-375L laser diode has been shown here. The inset represents the *Y*-axis in log scale to depict the differences at longer time.

were estimated, and it was found that τ_{rot} for Ag_9/HSA was much faster than that of Ag_{14}/HSA (Figure S2, SI). This could be ascribed to the smaller size of Ag_9/HSA, and also, the exceptionally high values of the residual anisotropy (r_∞) signify the constrained environments experienced by the fluorophores. Because the Ag/HSA NCs become embedded in the protein matrix and the chemical and physical properties of these bioconjugates are a function of their size, we performed matrix assisted laser desorption ionization-time of flight (MALDI-TOF) experiments. For HSA alone, the MALDI-TOF spectra is peaked at a m/z of 66430 Da, which is shifted to 67427 and 67988 Da for the Ag_9/HSA and Ag_{14}/HSA, respectively (Figure 3).

The differences of mass underscores the fact that in the absence of $NaBH_4$, 9 Ag atoms cluster to form the bioconjugate (Ag_9/HSA), whereas the presence of it makes the aggregation number increase to 14 (Ag_{14}/HSA). Transmission electron microscope (TEM) images also reveal that two types of NCs are indeed forming; the Ag_{14}/HSA are of a bigger size than that of the Ag_9/HSA NCs (Figure S3, SI).

Both the physical and chemical properties of the NCs can be tuned by monitoring the experimental conditions, and because the QYs as mentioned above are very high, these Ag/HSA NCs find tremendous chemical and biomedical applications.[24,25] In general, a mechanism similar to the biomineralization of inorganic ions by living organisms may be the driving force for the formation of these NCs. When $AgNO_3$ is added to HSA solution, the Ag^+ ions become entrapped inside of the various scaffolds inherently present in the protein and become stabilized via electrostatic interactions between the several functional groups like −OH, $-NH_2$, −COOH, and −SH present inside of the protein scaffolds.[1,14,26] These entrapped Ag^+ ions get stabilized due to the bulky nature of HSA and experience a constrained environment that in turn enhances its QY. The added NaOH so adjusts the pH, which enables the tyrosine amino acid residues to reduce the Ag^+ to Ag; this reduction is initiated by the phenolic groups, and the pH should be greater than the pK_a (10.46) of tyrosine.[3,27] This entire process seems to be slow, and hence, the formation of

dx.doi.org/10.1021/jz301733y | J. Phys. Chem. Lett. 2012, 3, 3605−3609

Table 1. Fluorescence Lifetime Parameters and QYs for the Various Ag/HSA NC Systems

system	a_1	τ_1 (ns)	a_2	τ_2 (ns)	a_3	τ_3 (ns)	$\langle\tau\rangle^a$ (ns)	χ^{2b}	QY^c (%)
Ag_9/HSA	26.8	2.35	63.2	10.8	10.0	0.47	7.51	1.13	16
Ag_{14}/HSA	42.4	1.71	36.8	5.18	20.8	0.45	2.72	1.06	11
Ag_9/HSA (converted)	28.0	2.60	60.8	11.54	11.2	0.50	7.80	1.17	15.4
Ag_{14}/HSA (converted)	41.0	1.67	35.7	6.17	23.3	0.39	2.98	1.08	9.8

$^a\langle\tau\rangle = (a_1\tau_1 + a_2\tau_2 + a_3\tau_3)/(a_1 + a_2 + a_3)$. $^b\chi^2$ denotes the goodness of the fitting. ^{c}QYs of the systems were calculated using fluorescein as a reference whose reported QY is 79% in ethanol (Kellog, R. E.; Bennett, R. G. Radiationless Intermolecular Energy Transfer III. Determination of Phosphorescence Efficiencies. *J. Chem. Phys.* **1964**, *41*, 3042−3045).

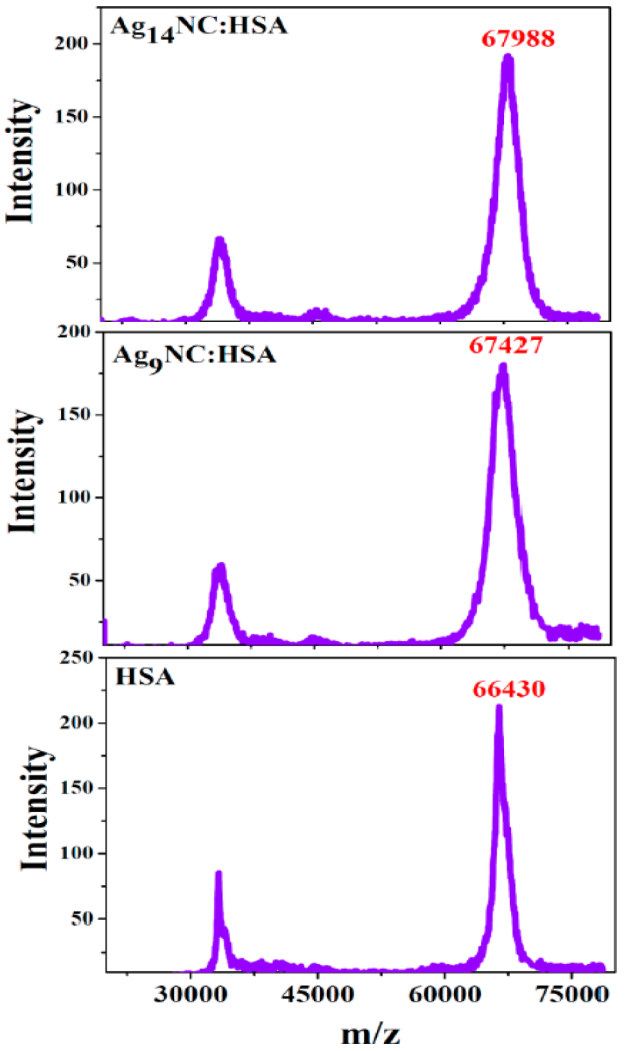

Figure 3. MALDI-TOF mass spectra of HSA (lower panel), Ag_9/HSA (middle panel), and Ag_{14}/HSA (upper panel).

the Ag_9/HSA takes around 10 h for completion (Scheme 1). The QY of the same system at 25 °C is about 9%, and this further underscores the importance of the synthesis because at physiological temperature (37 °C), the QY is higher (∼16%, Figure S4, SI). When $NaBH_4$ is added, its strong reducing properties overshadow those of tyrosine, and the embedded Ag^+ is reduced instantly, thereby resulting in the formation of Ag_{14}/HSA. Also, the $NaBH_4$ may enhance the aggregation of individual Ag atoms to a larger extent, which in turn leads to the formation of bigger NCs.

Besides synthesizing two NCs having varied physicochemical properties, we also demonstrate herein that these NCs are rapidly interconvertible (Scheme 1). By adding a strong

Scheme 1. Schematic Representation of the Formation and Interconversion of Ag_9/HSA and Ag_{14}/HSA

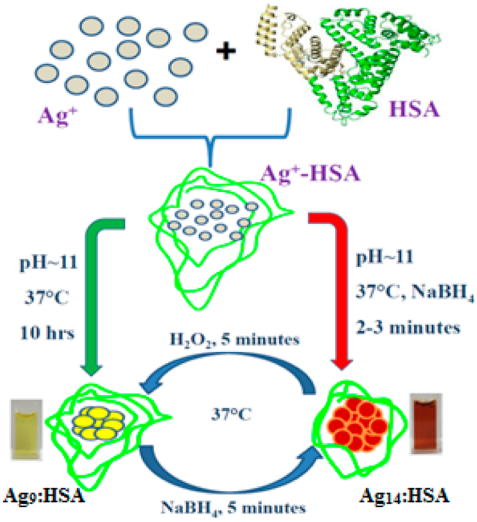

oxidizing agent, H_2O_2, the red-emitting Ag_{14}/HSA are fully converted to blue-emitting Ag_9/HSA NCs within 5 min. The emission properties, lifetimes, and QYs of these converted Ag_9/HSA are almost exactly similar to the separately synthesized Ag_9/HSA, as discussed earlier (Figure S5, SI and Table 1). Hence, despite not being a "green methodology", Ag_9/HSA can be prepared much faster by this simple oxidative conversion technique, contrary to what we experienced earlier where it took around 10 h. When $NaBH_4$ was added instead to the already synthesized Ag_9/HSA, we obtained red-emitting Ag/HSA NCs, having a broader emission peak at around 690 nm (Figure S6, SI). These species may have a multicomposition of higher aggregated Ag atoms besides Ag_{14}/HSA and are also characterized by high QYs, as encountered earlier. These newly formed red-emitting Ag/HSA are however fully convertible to Ag_9/HSA by the addition of H_2O_2, retaining all of their photophysical properties, which emphasizes the uniqueness of our strategies (Figures S7−S9, SI). Near-IR excitations are always less harmful to biological samples and have greater depth of sample penetration as compared to the UV or visible excitation regimes. Our Ag/HSA NCs show nonlinear optical properties (Figure S10, SI) having intense fluorescence, thereby exhibiting the property of two-photon excitation (λ_{ex} = 960 instead of 480 nm for Ag_{14}/HSA and λ_{ex} = 760 instead of 380 nm for Ag_9/HSA). This unique "up-converting" property of our synthesized Ag/HSA NCs will certainly find tremendous applications as photoluminescent stains for bioimaging and biolabeling. The nature of the excitation spectra of Ag_9/HSA and Ag_{14}/HSA NCs, as mentioned in Figure S10 (SI), is different. As mentioned earlier, the QY of Ag_9/HSA is higher than that of Ag_{14}/HSA; hence, the photoluminescent intensity

dx.doi.org/10.1021/jz301733y | J. Phys. Chem. Lett. 2012, 3, 3605−3609

of Ag_9/HSA is much higher than that of Ag_{14}/HSA. The excitation spectra of Ag_9/HSA are much simpler and smoother as compared to those of Ag_{14}/HSA. This may be due to some heterogeneity present within the Ag_{14}/HSA NCs. This heterogeneity may result in an increased asymmetry after cluster formation, which in turn may lead to such spectra having multiple peaks.

In addition, both Ag_9/HSA and Ag_{14}/HSA can be used in several areas of forensic sciences, which include security documentation and detecting counterfeiting, and can also be used as invisible inks. When used as markers on glass slides, both Ag_9/HSA and Ag_{14}/HSA cannot be viewed under ordinary white light, but interestingly, they emit blue and red fluorescence, respectively, when subjected to UV radiation (Figure S11, SI). Also, these Ag/HSA NCs can be effectively used in latent fingerprinting technology, where the hydrophobic surface housing the HSA helps in better adhesion of these NCs to the ridges of the finger marks, thereby enhancing the image intensity under UV light.[28] This property of our NCs enhances their prospects in biomedical diagnosis, where visualizing specific bio-organic components in forensic toxicology or pathology is essential.

In summary, to the best of our knowledge, this is the first report of a green one-pot synthesis of Ag/NCs using HSA as a template. The protein-induced synthesis of Ag_9/NCs and Ag_{14}/NCs has the highest QYs reported to date. The uniqueness of the work is that both NCs are interconvertible, whereby almost all of their photophysical properties are retained. Because the emission properties of these NCs can be tuned at will and as per our need, they find vast applications in biolabeling and imaging. The properties of two-photon excitation enable our Ag/HSA NCs to be used as fluorescence markers for delicate and sensitive biological samples. The extreme ease and low-cost synthetic procedures of these NCs will make them serve as unique photoluminescent tools, not only in chemistry and biology but also in forensic sciences.

■ ASSOCIATED CONTENT

Ⓢ Supporting Information

The detailed experimental procedures, instrumentation, and several spectra of the Ag/HSA nanoclusters showing their photophysical properties. This material is available free of charge via the Internet at http://pubs.acs.org.

■ AUTHOR INFORMATION

Corresponding Author

*E-mail: saptarshi@iiserb.ac.in.

Author Contributions

[§]Authors share equal contribution.

Notes

The authors declare no competing financial interest.

■ ACKNOWLEDGMENTS

We sincerely thank IISER Bhopal and the DST-Fast track scheme (No.: SR/FT/CS-19/2011) SERB for financial support and Mr. Arshad Akbar for helping us in finalizing the manuscript. S.M. thanks Dr. Sobhan Sen, SPS, JNU, New Delhi for many stimulating discussions. We also thank AIRF, JNU, New Delhi for helping us with the MALDI-TOF and TEM experiments. U.A. thanks CSIR, and S.G. thanks UGC, Govt. of India, for fellowships.

■ REFERENCES

(1) Guével, X. L.; Hötzer, B.; Jung, G.; Hollemeyer, K.; Trouillet, V.; Schneider, M. Formation of Fluorescent Metal (Au, Ag) Nanoclusters Capped in Bovine Serum Albumin Followed by Fluorescence and Spectroscopy. *J. Phys. Chem. C* **2011**, *115*, 10955−10963.

(2) Mohanty, J. S.; Xavier, P. L.; Chaudhari, K.; Bootharaju, M. S.; Goswami, N.; Pal., S. K.; Pradeep, T. Luminescent, Bimetallic AuAg Alloy Quantum Clusters in Protein Templates. *Nanoscale* **2012**, *4*, 4255−4462.

(3) Xie, J.; Zheng, Y.; Ying, J. Y. Protein-Directed Synthesis of Highly Fluorescent Gold Nanoclusters. *J. Am. Chem. Soc.* **2009**, *131*, 888−889.

(4) Derfus, A. M.; Chan, W. C. W.; Bhatia, S. N. Probing the Cytotoxicity of Semiconductor Quantum Dots. *Nano Lett.* **2004**, *4*, 11−18.

(5) Retnakumari, A.; Setua, S.; Menon, D.; Ravindran, P.; Muhammed, H.; Pradeep, T.; Nair, S.; Koyakutty, M. Molecular-Receptor-Specific, Non-Toxic, Near-Infrared-Emitting Au Cluster−Protein Nanoconjugates for Targeted Cancer Imaging. *Nanotechnology* **2010**, *21*, 055103.

(6) Dreaden, E. C.; Alkilany, A. M.; Huang, X.; Murphy, C. J.; El-Sayed, M. A. The Golden Age: Gold Nanoparticles for Biomedicine. *Chem. Soc. Rev.* **2012**, *41*, 2740−2779.

(7) Murphy, C. J.; Gole, A. M.; Stone, J. W.; Sisco, P. N.; Alkilany, A. M.; Goldsmith, E. C.; Baxter, S. C. Gold Nanoparticles in Biology: Beyond Toxicity to Cellular Imaging. *Acc. Chem. Res.* **2008**, *41*, 1721−1730.

(8) Huang, J.; Jackson, K. S.; Murphy, C. J. Polyelectrolyte Wrapping Layers Control Rates of Photothermal Molecular Release from Gold Nanorods. *Nano Lett.* **2012**, *12*, 2982−2987.

(9) Li, J.; Zhong, X.; Cheng, F.; Zhang, J.-R.; Jiang, L.-P.; Zhu, J.-J. Synthesis of Aptamer-Functionalized Silver Nanoclusters for Cell-Type-Specific Imaging. *Anal. Chem.* **2012**, *84*, 4140−4146.

(10) Zheng, J.; Nicovich, P. R.; Dickson, R. M. Highly Fluorescent Noble-Metal Quantum Dots. *Annu. Rev. Phys. Chem.* **2007**, *58*, 409−413.

(11) Zheng, J.; Zhang, C. W.; Dickson, R. M. Highly Fluorescent, Water-Soluble, Size-Tunable Gold Quantum Dots. *Phys. Rev. Lett.* **2004**, *93*, 077402.

(12) Yu, J.; Patel, S. A.; Dickson, R. M. In vitro and Intracellular Production of Peptide-Encapsulated Fluorescent Silver Nanoclusters. *Angew. Chem., Int. Ed.* **2007**, *46*, 2028−2030.

(13) Petty, J. T.; Zheng, J.; Hud, N. V.; Dickson, R. M. DNA-Templated Ag Nanocluster Formation. *J. Am. Chem. Soc.* **2004**, *126*, 5207−5212.

(14) Mathew, A.; Sajanlal, P. R.; Pradeep, T. A Fifteen Atom Silver Cluster Confined in Bovine Serum Albumin. *J. Mat. Chem.* **2011**, *21*, 11205−11212.

(15) Guo, W.; Yuan, J.; Dong, Q.; Wang, E. Highly Sequence-Dependent Formation of Fluorescent Silver Nanoclusters in Hybridized DNA Duplexes for Single Nucleotide Mutation Identification. *J. Am. Chem. Soc.* **2010**, *132*, 932−934.

(16) Richards, C. I.; Choi, S.; Hsiang, J.-C.; Antoku, Y.; Vosch, T.; Bongiorno, A.; Tzeng, Y.-L.; Dickson, R. M. Oligonucleotide-Stabilized Ag Nanocluster Fluorophores. *J. Am. Chem. Soc.* **2008**, *130*, 5038−5039.

(17) Xu, H.; Suslick, K. S. Sonochemical Synthesis of Highly Fluorescent Ag Nanoclusters. *ACS Nano* **2010**, *4*, 3209−3214.

(18) Tanaka, S. I.; Miyazaki, J.; Tiwari, D. K.; Jin, T.; Inouye, Y. Fluorescent Platinum Nanoclusters: Synthesis, Purification, Characterization, and Application to Bioimaging. *Angew. Chem., Int. Ed.* **2011**, *50*, 431−435.

(19) Negishi, Y.; Chaki, N. K.; Shichibu, Y.; Whetten, R. L.; Tsukuda, T. Origin of Magic Stability of Thiolated Gold Clusters: A Case Study on $Au_{25}(SC_6H_{13})_{18}$. *J. Am. Chem. Soc.* **2007**, *129*, 11322−11323.

(20) Negishi, Y.; Nobusada, K.; Tsukuda, T. Glutathione-Protected Gold Clusters Revisited: Bridging the Gap between Gold(I)−Thiolate Complexes and Thiolate-Protected Gold Nanocrystals. *J. Am. Chem. Soc.* **2005**, *127*, 5261−5270.

(21) Negishi, Y.; Takasugi, Y.; Sato, S.; Yao, H.; Kimura, K.; Tsukuda, T. Magic-Numbered Au_n Clusters Protected by Glutathione Monolayers (n = 18, 21, 25, 28, 32, 39): Isolation and Spectroscopic Characterization. *J. Am. Chem. Soc.* **2004**, *126*, 6518−6519.
(22) Adhikari, B.; Banerjee, A. Facile Synthesis of Water-Soluble Fluorescent Silver Nanoclusters and Hg^{II} Sensing. *Chem. Mater.* **2010**, *22*, 4364−4371.
(23) Michl, J.; Bonacic-Koutecky, V. *Electronic Aspects of Organic Photochemistry*; John Wiley & Sons, Inc.: New York, 1990.
(24) Yu, J.; Choi, S.; Dickson, R. M. Shuttle-Based Fluorogenic Silver-Cluster Biolabels. *Angew. Chem., Int. Ed.* **2009**, *48*, 318−320.
(25) Guével, X. L.; Spies, C.; Daum, N.; Jung, G.; Schneider, M. Highly Fluorescent Silver Nanoclusters Stabilized by Glutathione: A Promising Fluorescent Label for Bioimaging. *Nano Res.* **2012**, *5*, 379−387.
(26) Diéz, I.; Ras, H. A. Fluorescent Silver Nanoclusters. *Nanoscale* **2011**, *3*, 1963−1970.
(27) Xie, J.; Lee, J. Y.; Wang, D. I. C.; Ting, Y. P. Silver Nanoplates: From Biological to Biomimetic Synthesis. *ACS Nano* **2007**, *1*, 429−439.
(28) Sametband, M.; Shweky, I.; Banin, U.; Mandler, D.; Almog, J. Application of Nanoparticles for the Enhancement of Latent Fingerprints. *Chem. Commun.* **2007**, *43*, 1142−1144.